MIMO-Monopulse Target Localization for Automotive Radar

Feng, Ruoyu; Uysal, Faruk; Aubry, Pascal; Yarovoy, Alexander

DOI
10.1049/iet-rsn.2018.5013

Publication date
2018

Document Version
Final published version

Published in
IET Radar, Sonar and Navigation

Citation (APA)
Feng, R., Uysal, F., Aubry, P., & Yarovoy, A. (2018). MIMO-Monopulse Target Localization for Automotive Radar. *IET Radar, Sonar and Navigation*, *12*(10), 1131-1136. https://doi.org/10.1049/iet-rsn.2018.5013

IET Radar, Sonar & Navigation

Special Issue: Advanced Automotive Sensing – Towards Car Autonomy

MIMO–monopulse target localisation for automotive radar

ISSN 1751-8784
Received on 9th March 2018
Revised 26th July 2018
Accepted on 30th July 2018
E-First on 11th September 2018
doi: 10.1049/iet-rsn.2018.5013
www.ietdl.org

Ruoyu Feng[1], Faruk Uysal[1] ✉, Pascal Aubry[1], Alexandar Yarovoy[1]

[1]Faculty of Electrical Engineering, Mathematics and Computer Science, Delft University of Technology, 2600 AA Delft, Netherlands

✉ *E-mail: f.uysal@tudelft.nl*

Abstract: In this study, the authors propose a novel direction of arrival (DoA) estimation algorithm called 'multiple-input–multiple-output (MIMO)–monopulse' by combining the monopulse approach with MIMO radar. Monopulse is fast and accurate angle estimation algorithm, which has been well developed for tracking radar. The application of the monopulse technique on MIMO radar is not much considered before, especially for automotive-radar application, and will be discussed in this study. Conventional methods of monopulse DoA estimation include amplitude and phase comparison monopulse. In this study, to improve the performance of monopulse, they utilise Chebyshev and Zolotarev weighting to synthesise sum and difference patterns. A new visualisation method for monopulse ratio is discussed. Finally, they demonstrate the success of the proposed algorithm by processing real data from a 79 GHz frequency-modulated continuous-wave automotive radar.

1 Introduction

The research of autonomous driving is undergoing explosive development. Among all technologies applied to an autonomous driving car, different sensors, which are equal to 'eyes' of a vehicle, are utilised to sense the environment and locate the position of targets. The corresponding algorithms are required to provide the information for an autonomous car to determine strategies in different scenarios. The researches on sensors and target localisation algorithms have become a crucial topic for autonomous sensing.

Millimetre-wave radar is the most commonly used sensor for automotive-radar systems, which has been well developed in the past decades and widely used in current advanced driver assistance systems (ADASs). Compared to other sensors used in ADAS such as camera and light detection and ranging, millimetre-wave radar has the advantages of robust performance against low-vision conditions even severe weather. Thus, automotive radar is the key element for ADAS and future autonomous driving systems.

The most common modulation method for automotive radar is to transmit frequency-modulated continuous-wave (FMCW) waveforms to detect the range and velocity of targets through deramp processing [1]. In addition, multiple-input–multiple-output (MIMO) radar utilises an antenna array with multiple elements to provide the angular information, and direction of arrival (DoA) estimation is a significant issue for target localisation.

Conventional DoA estimation algorithms include parametric and non-parametric methods. Non-parametric methods such as` deterministic and stochastic maximum-likelihood (DML and SML) approaches have nice performance but have to solve non-linear multi-dimensional optimisation problems [2, 3]. Parametric methods include beamforming and subspace-based algorithms, which localise the DoA by searching the maximum point of the spectrum [4]. Beamforming is one of the basic DoA algorithms which maximises the output signal to a specific direction using a weight vector. Subspace-based method also called super-resolution algorithms such as multiple signal classfication (MUSIC) and estimation of signal parameters via rotational invariant techniques (ESPRIT), which utilise eigenstructure analysis, can improve the estimation performance but suffer when few measurements (snapshot) are available [5, 6]. All these methods are based on eigenstructure analysis which requires correct source number estimation to determine the effective rank of a correlation matrix. Moreover, super-resolution algorithms are computationally expensive, thus they are not suitable for real-time automotive-radar applications.

Compared to subspace-based algorithms, monopulse has potential benefits of saving computation cost, having fewer requirements (no need to know the number of targets) and capability to work using single snapshot. Monopulse has better angle determination accuracy than the conventional digital beamforming (DBF) to localise the maximum of the beam scanning pattern for DoA estimation, and it naturally provides benefits in target tracking radar systems [7, 8].

The concept of combining MIMO and monopulse (MIMO–monopulse) has been studied in the literature [9] but most of them utilise distributed MIMO with widely separated transmitters and receivers, whereas collocated MIMO–monopulse has not been fully exploited. In [10–12], the mathematical models of amplitude and phase comparison monopulse (PCM) on MIMO radar are discussed but none of these algorithms are verified by actual radar experiment, and the synthesis of sum and difference beam pattern is not considered.

In this paper, a novel angle estimation algorithm based on monopulse is proposed for collocated MIMO radar and validated by a real automotive-radar measurement (primary work has been finished in [13]). Section 2 discusses the signal model of MIMO radar. The implementation of MIMO–monopulse algorithms is proposed in Section 3, synthesis of sum and difference beam patterns is considered, and target tracking using MIMO–monopulse is discussed in Section 4. In Section 5, the MIMO–monopulse algorithm is validated using simulated and experimental data sets. Finally, recommendations and possible future work are discussed in Section 6.

2 Signal model and DoA estimation

The concept of automotive FMCW radars is to measure the difference frequency (or beat frequency) between the transmitted and received signals to obtain the range and velocity information [14]. First a chirp signal

$$s(t) = \mathrm{e}^{\mathrm{j}2\pi((k/2)t^2)}, \quad 0 \le t \le T \tag{1}$$

is generated in the intermediate frequency, where k is the slope and T is the duration of the reference signal. The baseband signal is modulated with a carrier signal f_c and transmitted through free space, which is expressed as

$$s_T(t) = e^{j2\pi((k/2)t^2 + f_c t)}. \tag{2}$$

Note that, a transmitted signal is a real-valued signal $\mathrm{Re}\{s_T(t)\}$. We use a complex form of analytical signals in this paper for the convenience of analysis. The received signal is a delayed replica of the transmitted signal which can be written as

$$s_R(t) = e^{j2\pi((k/2)(t-\tau)^2 + f_c(t-\tau))}. \tag{3}$$

The delay between the transmitted and received signals τ can be calculated as $\tau = 2(R + vt)/c$, where c is the speed of light, R and v are the range and the line-of-sight velocity of the target, respectively.

The basic processing of FMCW signals is called deramp processing, which is defined as multiplying the complex conjugate of the received signal with the transmitted one (also known as the reference signal). The output of deramping, the beat signal can be written as

$$\begin{aligned} s_{\text{beat}}(t) &= s_T(t)\, s_R^*(t) \\ &= e^{j2\pi(k\tau t - (k/2)\tau^2 + f_c\tau)} \\ &\simeq e^{j2\pi\left((2f_c R/c) + ((2f_c v/c) + (2kR/c))t + (2kv/c)t^2\right)} \end{aligned} \tag{4}$$

where the term of $\tau^2 = 4(R + vt)^2/c^2 \simeq 0$. Bearing in mind that the last term of phase can also be neglected $[(2kv/c)t^2 \simeq 0]$, the beat frequency of the FMCW signal can be defined as

$$f_b = \frac{2f_c v}{c} + \frac{2kR}{c}. \tag{5}$$

This beat frequency includes both range and Doppler (velocity) information regarding the targets, which is obtained through a fast Fourier transform (FFT) on fast-time samples of beat signals, and then range can be calculated by f_b. The transmitter repeatably generates FMCW signal ramps, which provides velocity information due to Doppler effect. To obtain the Doppler frequency f_D, the two-dimensional (2D) FFT should be adopted on slow-time samples. The peak of the 2D-FFT spectrum will appear at

$$[f_b, f_D] = \left[\frac{2kR}{c}, \frac{2vf_c}{c}\right]. \tag{6}$$

The target localisation requires both the range and bearing information. Suppose the FMCW automotive radar utilises uniform linear array to localise the azimuth of targets. Consider there are M_T transmitters and M_R receivers in a collocated MIMO antenna array. The azimuth of targets can be estimated in MIMO because the line-of-sight direction of the radar waveform can be regarded as parallel under far-field configuration. Thus, the front of the transmitted waveform reaches the target and the echo signal reflected each receiver in the array with consecutive increasing time delay. The time delay can be approximated as a phase shift if the transmitted signal is a narrow band [15].

Suppose that the transmitted signals at each transmitter are $\boldsymbol{s}_i$, $i = 1, \ldots, M_t$, which is orthogonal to each other in a snapshot. Each receiver element in antenna receive signals generated by all transmitters, thus there are $M = M_t \times M_r$ collected channels in the MIMO configuration which can be exploited by a virtual array model. Such that, the transmitter $\boldsymbol{a}_T$ and receiver $\boldsymbol{a}_R$ steering vectors in the direction of θ indicates the phase delay of each element in an antenna array and are expressed as

$$\begin{aligned} \boldsymbol{a}_T(\theta) &= \begin{bmatrix} 1 & e^{j2\pi(d_T/\lambda)\sin(\theta)} & \cdots & e^{j2(M_T-1)\pi(d_T/\lambda)\sin(\theta)} \end{bmatrix}^T \\ \boldsymbol{a}_R(\theta) &= \begin{bmatrix} 1 & e^{j2\pi(d_R/\lambda)\sin(\theta)} & \cdots & e^{j2(M_R-1)\pi(d_R/\lambda)\sin(\theta)} \end{bmatrix}^T \end{aligned} \tag{7}$$

where λ is the wavelength; d_T and d_R are the inter-element spacing of the transmitters and the receivers, respectively. The steering vector of the virtual array is formulated through Kronecker product of transmitter and receiver array steering vectors

$$\boldsymbol{a}(\theta) = \boldsymbol{a}_T(\theta) \otimes \boldsymbol{a}_R(\theta). \tag{8}$$

To avoid grating lobes in the beam pattern of virtual steering vectors, the distance between two virtual elements has to be no larger than $\lambda/2$, which requires the d_T and d_R to be configured properly. Then, the received MIMO signal model is expressed as

$$\boldsymbol{x}(t) = \sum_{i=1}^{K} \beta_i \boldsymbol{a}_i(\theta) \boldsymbol{s}_i(t-\tau) + n(t) \tag{9}$$

where β_i is the amplitude of the ith target source, $\boldsymbol{a}_i(\theta)$ is the steering vector of the virtual array, $\boldsymbol{s}_i(t-\tau)$ is the received signal, and $n(t)$ is the white noise assumed to be spatially independent and identically distributed . If the radar received L snapshots of the signal, 3D data $\boldsymbol{X}(t) = [\boldsymbol{x}_1(t), \ldots, \boldsymbol{x}_L(t)]$ is collected. The signal $\boldsymbol{X}(t)$ can be deramped and processed by 2D-FFT on fast-time and slow-time dimensions to obtain a range–Doppler map, and then the DoA of targets can be reached by the algorithms on the spatial domain.

3 DoA estimation using MIMO–monopulse

The monopulse technique is based on delay-and-sum beamforming or conventional beamforming. The DBF technique steers the signal to the desired direction through changing the weight of each channel of the signal, which output can be written as

$$y = \boldsymbol{w}^H \boldsymbol{x} \tag{10}$$

where $\boldsymbol{w}$ is the weighting vector and $\boldsymbol{x}$ is the signal to be processed. The DoA estimation using DBF is realised by searching the maximum of the DBF response pattern, which is located at the direction of steering θ. The pattern is expressed as

$$P(\theta) = \boldsymbol{w}^H \boldsymbol{a}(\theta), \tag{11}$$

where $\boldsymbol{a}(\theta)$ is the steering vector [4]. Collocated MIMO radar systems use a virtual array to generate sum and difference beams, which are utilised by the DBF. Then, DoA can be determined by computing the monopulse ratio, which is defined as the ratio of the difference to sum beamforming output. It should be noted that unlike classical monopulse approach, we propose to synthesise monopulse beams through MIMO virtual array, which takes the advantage of both transmit and receive array elements.

For amplitude comparison monopulse, the left and right beams are generated by two beamforming vectors centred at a look direction θ_0 but separated by a squint angle shift θ_s to left and right [16]. The difference of voltage of the left and right beams will be zero if the target is precisely located at θ_0. For PCM, the antenna array can be divided into two equal sub-arrays to compare phase information. Consider an array of M elements. The left $M/2$ elements consist of left sub-array while the rest of the elements consists of the right one [11]. Define the weights of left and right beamformers as $\boldsymbol{w}_l$ and $\boldsymbol{w}_r$, the ACM beamforming weights of left and right beams are given by $\boldsymbol{w}_l = \boldsymbol{a}(\theta_0 - \theta_s/2)$ $\boldsymbol{w}_r = \boldsymbol{a}(\theta_0 + \theta_s/2)$. After beamforming using left and right weighting vectors, the voltage of the two beams is compared with location of the angle of the targets. The difference between the two beams is 0, only when the target is in the look direction θ_0.

If we consider the phase information of the beam, the virtual array can be divided into two sub-arrays. Unlike amplitude comparison, the left and right beamforming vector weights are defined for two sub-arrays. Consider a virtual array of M elements, the left $M/2$ elements consists of left sub-array while the rest of the elements consists of the right one. Left and right beams are generated by first and second sub-arrays separately, and the weight vectors are defined as $\boldsymbol{w}_1$ and $\boldsymbol{w}_2$, which both have the lengths of

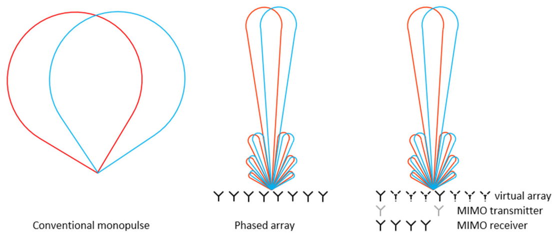

Fig. 1 *Traditional monopulse versus phase array monopulse versus MIMO monopulse*

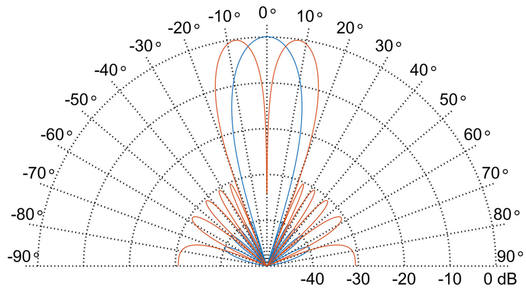

Fig. 2 *Sum (Chebyshev) and difference (Zolotarev) beam pattern of the proposed synthesis*

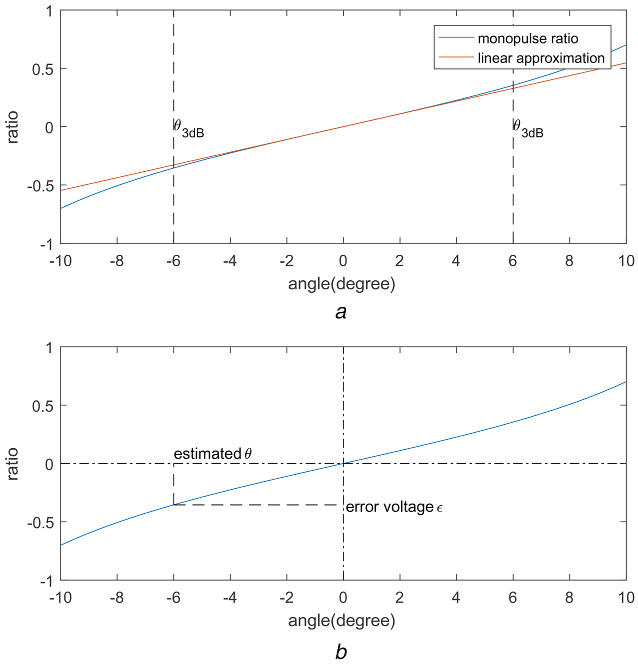

Fig. 3 *Monopulse ratio curve and 3 dB local region*
(a) Linear approximation, ***(b)*** Error voltage and inverse mapping

$M/2$. When the target is in the look direction of the array, the phase difference will be exactly 0.

The comparison of conventional monopulse phased array monopulse and MIMO–monopulse (amplitude comparison method) is illustrated in Fig. 1. The conventional monopulse generates left and right beams using two separate horns which are slightly squinted to left and right, while the phased array monopulse and MIMO–monopulse realise it through beamforming on antenna array. The main difference between a phased array and an MIMO monopulse is that MIMO–monopulse implements left and right beam patterns on a virtual array but the phased array radar forms the beams directly on a physical array.

To further improve the performance of MIMO–monopulse, we propose a novel method to synthesise sum and difference beam pattern. The goal of the synthesis is to satisfy some requirements of beam patterns by changing the weighting of each element. For MIMO–monopulse, the sum pattern needs to maximise the gain and reduce the sidelobe, while for difference pattern, the first null beamwidth should be minimised and the normalised difference slope on the boresight should be maximised.

The Dolph–Chebyshev weighting of sum pattern provides the narrowest first null beamwidths for a specified sidelobe level or the minimum sidelobe level given a null-to-null mainlobe beamwidth. In the sense of Chebyshev weighting, Zolotarev weighting for difference pattern generates the excitation coefficients to obtain both the narrowest first null beamwidth and sharpest difference slope on the look direction of the beam [17]. Implementation of the Zolotarev polynomial requires knowledge of elliptic integrals, Jacobi moduli, and Jacobi eta, zeta, and elliptic functions, which is complex to realise. In [18], a close approximation to the Zolotarev pattern is realised through multiplying the Chebyshev pattern with an antisymmetric function, which can generate the Zolotarev pattern with 30 dB peak-to-sidelobe ratio with respect to the Chebyshev pattern with 40 dB, as is illustrated in Fig. 2.

The sum beam output will be maximum when the target is in the look direction θ_0, and the difference beam output will be zero. Thus, the monopulse ratio will be exactly zero when the target is located at the direction of the beam. If the target has a small offset angle from the look direction $(\theta - \theta_0)$, the error voltage is used to estimate this angle. The *error voltage* is computed by taking either the real part or imaginary part of the sum to difference output, which depends on the method of generating sum and difference beams [19]. For the proposed synthesis of the beam pattern, we use the imaginary part to compute error voltage ϵ

$$\epsilon = \Im\left\{\frac{\boldsymbol{w}_\Delta^{\mathrm{H}}\boldsymbol{x}}{\boldsymbol{w}_\Sigma^{\mathrm{H}}\boldsymbol{x}}\right\} \tag{12}$$

where $\boldsymbol{w}_\Delta$ and $\boldsymbol{w}_\Sigma$ are the weight vectors of difference and sum beam patterns, respectively. Once an error voltage is computed, the angle of the target is estimated through the monopulse ratio. An ideal monopulse ratio is defined as

$$R = \Im\left\{\frac{\boldsymbol{w}_\Delta^{\mathrm{H}}\boldsymbol{a}(\theta)}{\boldsymbol{w}_\Sigma^{\mathrm{H}}\boldsymbol{a}(\theta)}\right\} \tag{13}$$

Fig. 3 shows the linear approximation region of the monopulse to estimate the angle $\hat{\theta}$ through a linear mapping, which is expressed as

$$\hat{\theta} = \theta_0 - \gamma^{-1}\epsilon \tag{14}$$

where γ is the constant slope of monopulse ratio.

The estimation performance of the MIMO–monopulse using (14) is an approximation derived from maximum-likelihood estimator [8] but requires much less computational cost compared with conventional beam scan method for angle estimation.

4 Implementation and target tracking using MIMO–monopulse

As we discussed in the previous section, MIMO–monopulse realises fast and accurate angle estimation through (14) within the local linear approximation area. To implement the algorithm for the whole field of view (FOV) in the automotive-radar application, multiple monopulse beams can be generated simultaneously to cover the wide region, as is shown in Fig. 4. The FOV will be divided into several subareas, in which the azimuth of the target can be estimated by MIMO–monopulse. First, the angle is roughly estimated by DBF to determine in which beam the target is located (the red beam in Fig. 4), then the exact angle will be precisely calculated using MIMO–monopulse, as is illustrated in Fig. 4 using black dash.

In addition to precise DoA estimation, one advantage of MIMO–monopulse is that it can be utilised for target tracking. Consider a moving target to be localised, after estimating the angle of the target through MIMO–monopulse in one pulse of signals, sum and difference beams are obtained. For the next pulse of signals, if the angle of the target is shifted slightly, we can estimate

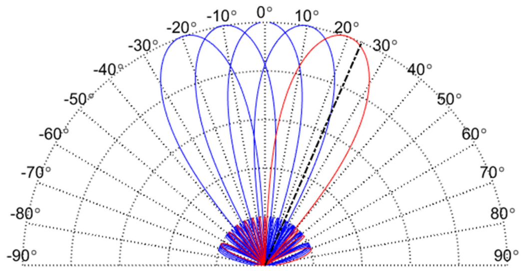

Fig. 4 *MIMO–monopulse scan by generating multiple beams simultaneously. Target is at 23° within the red beam steered to 20°*

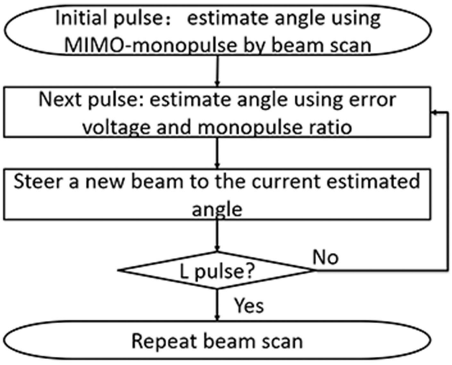

Fig. 5 *Flowchart of tracking the angle of the target using MIMO–monopulse*

the angle of the target for tracking purpose without full beam scan using the monopulse ratio, which is generated from previous sum and difference weighting vectors. Note that new beam steering is needed after a certain amount of time, especially target angle is moved out of the linear region. To keep tracking the angle of the target, a new beam is steered to the current direction of the target by generating new sum and difference weighting vectors. The steps above can be repeated for several pulses to track the angle of the target until another new beam scan is made in case there exist new targets in the FOV. The procedure of target tracking using MIMO–monopulse is illustrated in Fig. 5. It should be noted that the number of full beam scan is dramatically reduced by assuming the angle shift between two adjacent pulses, which can be estimated using monopulse ratio, are quite small to guarantee the direction of the target keeps located within the linear approximation region of monopulse beam.

When the MIMO–monopulse algorithm is used to realise azimuth tracking of the target, the proposed synthesis of the sum and difference beams improves the performance of monopulse angle estimation, as shown in Fig. 6. It can be seen that compared with conventional amplitude and PCM, a better local region of linear approximation is generated, which has lower estimation error when the angle of a target is shifted to the direction of the beam that reduces the number of new beam steering.

5 Experiments

The proposed algorithm is first implemented through MATLAB and then validated on the actual automotive radar. As is discussed in Section 3, the DoA estimation is realised through searching the zero crossing of monopulse ratio. The output of the monopulse ratio is not straightforward to be visualised such as the response pattern of DBF (see in Fig. 7). To demonstrate the monopulse ratio in a range–azimuth map, we utilise a simple processing to map the monopulse ratio to dB scale and take the inverse, which generates a peak at the direction of a target.

Another issue needs to be solved is *monopulse ambiguity*. Since the MIMO radar transmitter element is omnidirectional and signals from all directions in a wide FOV are received, in monopulse output not only the response of targets within the mainlobe but also sidelobes generate zero crossings in monopulse ratio, which leads to an ambiguity to discriminate targets, as is shown in Fig. 7*a*. To

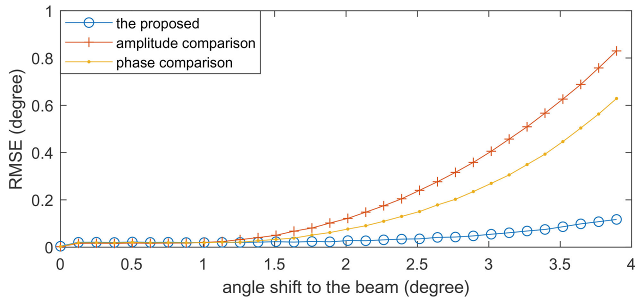

Fig. 6 *Estimation error of monopulse when tracking the angle of the target (L = 32 pulses after the first beam scan)*

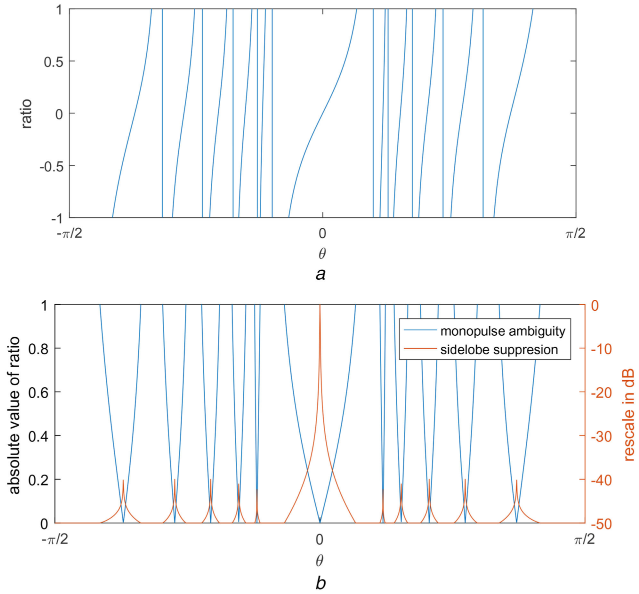

Fig. 7 *Monopulse ratio ambiguity and the proposed processing to resolve the ambiguity*

(a) Monopulse ratio ambiguity, ***(b)*** Absolute value and rescaled into dB

solve this ambiguity, in MIMO–monopulse, the monopulse ratio from sidelobes needs to be suppressed.

The approach to visualise the output of the monopulse ratio and resolve monopulse ambiguity is as follows. Assume there is a target at 0°, if we take the absolute value of monopulse ratio, then zero crossings of the monopulse ratio will become local minimum points (Figs. 7*a* and *b*). First, the absolute value of monopulse ratio is mapped into the dB scale and the negative of it is taken to generate narrow peaks, which are infinite large at the directions of the mainlobe and sidelobes. A dynamic range of 50 dB is taken for illustration purpose, which is shown in Fig. 7*b*.

In practise, dynamic range should be selected according to the dynamic range of the radar under application. To suppress sidelobes, we multiply this output with a window function. The window function is derived from the sum pattern in Fig. 2, which spans over [−50, 0] dB and normalised to a scalar as [0, 1]. As is shown in Fig. 7*b*, after processing by mapping and window function, we obtain a result to visualise the result of MIMO–monopulse, which is on the same scale with the DBF response pattern. The proposed processing above is only used for the visualisation in a range–azimuth map but not the actual procedure to realise the algorithm for target detection and tracking. Then, it is possible to demonstrate monopulse ratio in a range–azimuth map similar to the response pattern of DBF for an intuitive observation of the result using the proposed MIMO–monopulse algorithm. The tracking performance of the proposed synthesis of sum and difference pattern is simulated and compared with conventional amplitude and PCM (Fig. 6). It can be seen that through using Chebyshev and Zolotarev weighting, a better linear approximation region is obtained to estimate the DoA of targets with less estimation error.

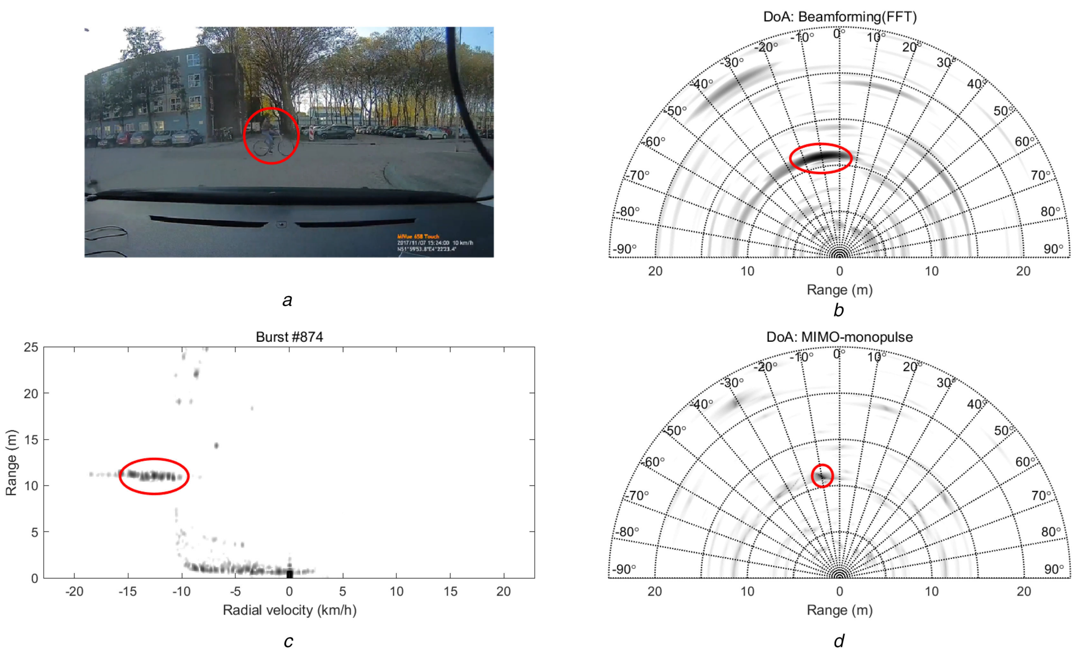

Fig. 8 *Range–Doppler map and range–azimuth map using conventional DBF and MIMO–monopulse, the position of the target is manually labelled using red oval, where the dynamic range is set to 30 dB for all corresponding sub-figures*
(a) Video record, ***(b)*** Range–Doppler map, ***(c)*** Range–azimuth map using beamforming (FFT), ***(d)*** Range–azimuth map using MIMO–monopulse

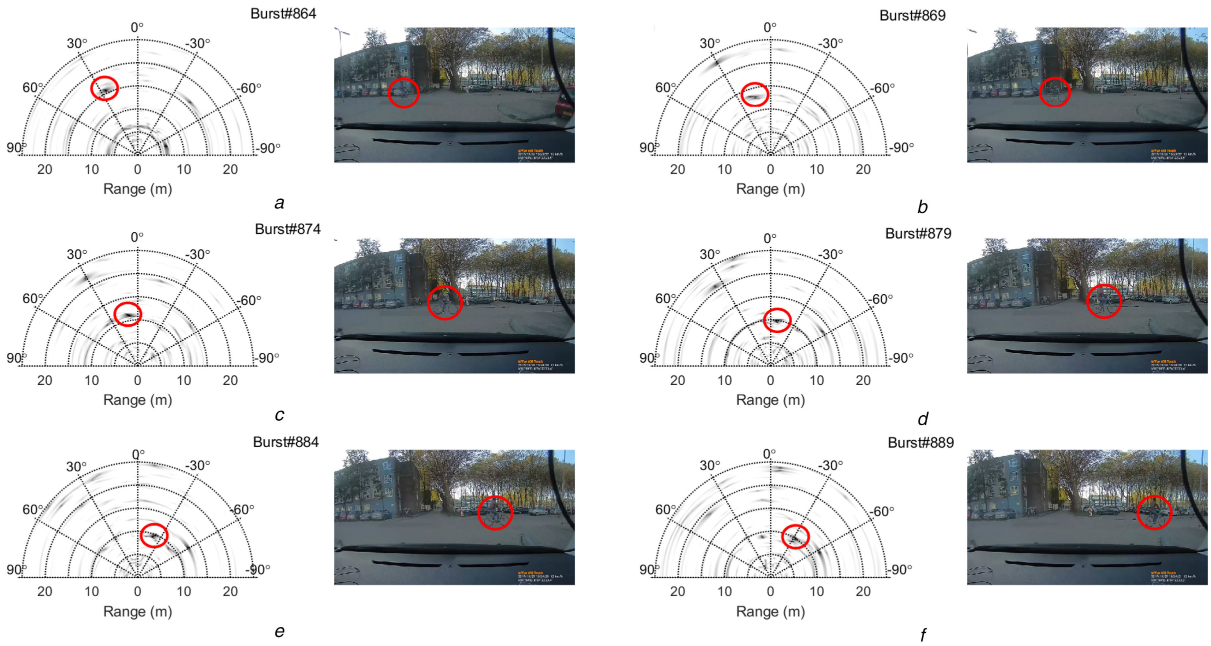

Fig. 9 *Range–azimuth map using MIMO–monopulse of a moving bicycle in six frames of the video at https://youtu.be/6BvSMn1yS9U. The target is manually labelled using red oval. Automatic real-time tracking is in progress*

To demonstrate the proposed method, an experimental testbed was prepared by using actual 79 GHz radar chip. The tested NXP Dolphin automotive radar has MIMO antenna arrays, which consist of three transmitters and four receivers to synthesise a 12-channel virtual array. First, the virtual array is calibrated by using a known source at 0° to compensate for the amplitude and phase error of the steering vector. Mutual coupling effect is not considered during the calibration since the mutual coupling between array elements is measured negligibly small. Experimental data was collected for an urban driving scenario to demonstrate the detection accuracy of the proposed MIMO–monopulse approach. As a reference to actual targets, a camera is used to record the video during the measurement. It should be noted that all data sets were collected in a moving platform (vehicle). The range–Doppler and range–azimuth maps of the burst 874 are shown in Fig. 8, and the corresponding frame of the video recording is given in Fig. 8*a*. Fig. 8*b* shows the distance and radial velocity of the target to the radar. DoA estimation using conventional beamforming and MIMO–monopulse are compared in Figs. 8*c* and *d*. A target of a bicycle is located at around $[11\text{m}, -10^{\circ}]$, and moving toward the right-hand side. In the range–azimuth map using beamforming, the angle of the target is difficult to be precisely determined due to the mainlobe beamwidth. However, after using our proposed algorithm, the DoA of the target is accurately localised by a sharp and narrow peak in the angular axis. In Fig. 9, the range–azimuth maps of the moving bicycle is shown in consecutive frames of the video, where the target is able to be easily discriminated. Compared to conventional DBF which has a wide mainlobe beamwidth limited by the number of sensors, the proposed MIMO–monopulse is able to localise the motion of the small targets such as pedestrian and bicycle, since monopulse is really sensitive to the azimuth shift.

6 Conclusion

In this paper, a quick and precise DoA estimation algorithm through combining monopulse technique with MIMO radar is proposed, which we call MIMO–monopulse. The ambiguity of applying monopulse on MIMO radar is resolved, and the output of MIMO–monopulse ratio is visualised in a similar approach to the DBF response pattern through mapping and window function, which can be demonstrated in a range–azimuth map. The proposed MIMO–monopulse algorithm indicates more accurate azimuth determination since it generates a sharp peak precisely located at the direction of a target. It is sensitive to the motion of small targets in the angular axis, which can be utilised for tracking targets such as pedestrian and bicycle. In addition, the synthesis of sum and difference pattern using Chebyshev and Zolotarev weighting is applied for generating better linear approximation local region, which provides better estimation accuracy when tracking the azimuth of the target.

The proposed method has been validated through processing actual radar data sets that collected from an outdoor driving experiment by using a 79 GHz FMCW automotive radar. The proposed MIMO–monopulse has shown improvement on localising the DoA of targets precisely compared with conventional DBF. The tracking performance of MIMO–monopulse is only simulated and will be applied to actual radar data in the next step. As for future work, the proposed method can be extended to a different application such as space–time adaptive processing, in order to suppress clutter (stationary object) and interference (mutual interference between different automotive radars) for better moving target detection. Moreover, for MIMO radar, the topology of transmitt and receive elements in the antenna array can be optimised to satisfy the specified requirements to improve the performance of the monopulse technique for DoA estimation [20, 21].

7 Acknowledgment

The authors gratefully acknowledge the hardware support from the NXP Semiconductors N.V. Netherlands.

8 References

[1] Winkler, V.: 'Range Doppler detection for automotive FMCW radars'. Microwave Conf. 2007 European, 2007, pp. 1445–1448

[2] Bohme, J.: 'Estimation of source parameters by maximum likelihood and nonlinear regression'. IEEE Int. Conf. ICASSP'84 Acoustics, Speech, and Signal Processing, vol. **9**, 1984, pp. 271–274

[3] Jaffer, A.G.: 'Maximum likelihood direction finding of stochastic sources: a separable solution'. 1988 Int. Conf. Acoustics, Speech, and Signal Processing 1988 ICASSP-88, 1988, pp. 2893–2896

[4] Van Trees, H.L.: '*Optimum array processing: part IV of detection, estimation, and modulation theory*' (John Wiley & Sons, New York, 2004)

[5] Schmidt, R.: 'Multiple emitter location and signal parameter estimation', *IEEE Trans. Antennas Propag.*, 1986, **34**, (3), pp. 276–280

[6] Roy, R., Kailath, T.: 'ESPRIT-estimation of signal parameters via rotational invariance techniques', *IEEE Trans. Acoust. Speech Signal Process.*, 1989, **37**, (7), pp. 984–995

[7] Sherman, S.M., Barton, D.K.: '*Monopulse principles and techniques*' (Artech House, Norwood, 2011)

[8] Nickel, U.: 'Overview of generalized monopulse estimation', *IEEE Aerosp. Electron. Syst. Mag.*, 2006, **21**, (6), pp. 27–56

[9] Gogineni, S., Nehorai, A.: 'Target tracking using monopulse MIMO radar with distributed antennas'. Radar Conf. 2010, 2010, pp. 194–199

[10] He, Q., He, Z., Li, H.: 'Multibeam amplitude comparison problems for MIMO radar's angle measurement'. Conf. Record of the 41st Asilomar Conf. Signals, Systems and Computers, 2007 ACSSC 2007, 2007, pp. 2163–2167

[11] Zhang, J., Liu, H., Li, J., *et al.*: 'Research on the mono-pulse phase comparison angle measurement algorithm of MIMO radar'. Int. Workshop Microwave and Millimeter Wave Circuits and System Technology (MMWCST), 2012, pp. 1–4

[12] Ito, T., Hirata, K., Takahashi, R.: 'Transmitting phase comparison monopulse estimation using MIMO radar technique for distributed array'. 2012 Int. Symp. Antennas and Propagation (ISAP), 2012, pp. 78–81

[13] Babur, G., Krasnov, O.A., Yarovoy, A., *et al.*: 'Nearly orthogonal waveforms for MIMO FMCW radar', *IEEE Trans. Aerosp. Electron. Syst.*, 2013, **49**, (3), pp. 1426–1437

[14] Feng, R., Uysal, F., Yarovoy, A.: 'Target localisation using MIMO–monopulse: application on 79 GHz automotive radar'. Radar Conf. (EURAD) 2018 European

[15] Van Veen, B.D., Buckley, K.M.: 'Beamforming: a versatile approach to spatial filtering', *IEEE ASSP Mag.*, 1988, **5**, (2), pp. 4–24

[16] An, C., Yang, J., Ran, R., *et al.*: 'Enhanced monopulse MIMO radar using reliable αβ filtering'. Military Communications Conf. 2012-MILCOM, 2012, pp. 1–6

[17] McNamara, D.: 'Direct synthesis of optimum difference patterns for discrete linear arrays using Zolotarev distributions', *IEEE Proc. H, Microw. Antennas Propag.*, 1993, **140**, (6), pp. 495–500

[18] Willis, A., Baker, C.: 'Approximation to Zolotarev polynomial ideal difference beams for linear arrays', *Electron. Lett.*, 2006, **42**, (10), pp. 561–563

[19] Seliktar, Y., Williams, D.B., Holder, E.J.: 'A space/fast-time adaptive monopulse technique', *EURASIP J. Adv. Signal Process.*, 2006, **2006**, (1), p. 014510

[20] Ito, T., Takahashi, R., Hirata, K.: 'An antenna arrangement for phase comparison monopulse DOA estimation using nonuniform planar array'. Radar Conf. (EuRAD) 2011 European, 2011, pp. 277–280

[21] Zhuge, X., Yarovoy, A.: 'Sparse multiple-input multiple-output arrays for high-resolution near-field ultra-wideband imaging', *IET Microw. Antennas Propag.*, 2011, **5**, (13), pp. 1552–1562